UNIVERSITY OF CALIFORNIA, BERKELEY
Department of Materials Science and Mineral Engineering

Final Technical Report
to
U.S. Air Force Office of Scientific Research/NA
on

MICROMECHANISMS OF FRACTURE AND FATIGUE-CRACK GROWTH IN BULK METALLIC GLASS ALLOYS
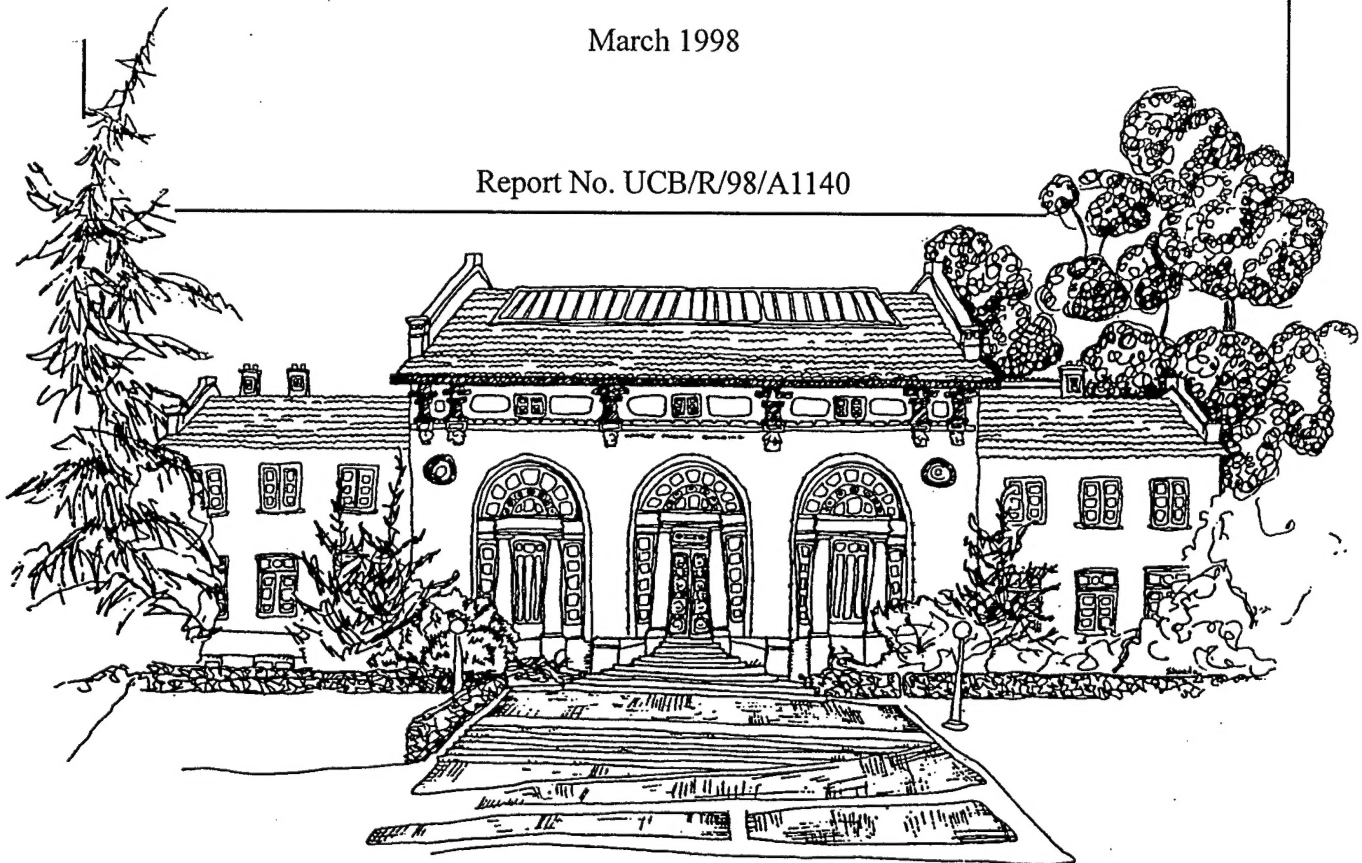
Grant No. F49620-97-1-0365

for period 1 May 1997 to 31 December 1997

by

C. J. Gilbert and R. O. Ritchie

March 1998

Report No. UCB/R/98/A1140

Hearst Mining Building, Berkeley, CA 94720-1760

AFRL-SR-BL-TR-98

REPORT DOCUMENT PAGE

0324

1. AGENCY USE ONLY (Leave blank)	2. REPORT DATE March 10, 1998	3. REPORT TYPE AND DATES COVERED Final Report: 1 May 97 – 31 Dec. 97

4. TITLE AND SUBTITLE
Micromechanisms of Fracture and Fatigue-Crack Growth in Bulk Metallic Glass Alloys

5. FUNDING NUMBERS

6. AUTHOR(S)
Christopher J. Gilbert and Robert O. Ritchie

7. PERFORMING ORGANIZATION NAME(S) AND ADDRESS(ES)
University of California, Berkeley
463 Evans Hall # 1760
Berkeley, CA 94720-1760

8. PERFORMING ORGANIZATION REPORT NUMBER
UCB/R/98/A1140

9. SPONSORING/MONITORING AGENCY NAME(S) AND ADDRESS(ES)
AFOSR/NA
110 Duncan Avenue, Suite B115
Bolling AFB, DC 20332-0001

10. SPONSORING / MONITORING AGENCY REPORT NUMBER
F49620-97-1-0365

11. SUPPLEMENTARY NOTES

12a. DISTRIBUTION / AVAILABILITY STATEMENT
Approved for public release; distribution is unlimited.

DTIC QUALITY INSPECTED

12b. DISTRIBUTION CODE

13. ABSTRACT (Maximum 200 words)

The recent development of metallic alloy systems which can be processed with an amorphous structure over large dimensions, specifically to form metallic glasses at low cooling rates (~10 K/s), has permitted novel measurements of important mechanical properties. These include, fatigue-crack growth and fracture toughness behavior, representing the conditions governing the subcritical and critical propagation of cracks. In the present study, bulk plates of a $Zr_{41.2}Ti_{13.8}Cu_{12.5}Ni_{10}Be_{22.5}$ alloy, machined into 7 mm thick, 38 mm wide compact-tension specimens and fatigue precracked following standard procedures, revealed fracture toughnesses in the fully amorphous structure of $K_{Ic} \sim 55$ MPa$\sqrt{m}$, i.e., comparable with that of a high-strength steel or aluminum alloy. However, annealing to induce partial and full crystallization was found to result in a drastic reduction in fracture toughness to ~1 MPa$\sqrt{m}$, i.e., comparable with silica glass. Under cyclic loading, whereas crack-propagation behavior of the bulk amorphous metal was similar to that observed in traditional steel and aluminum alloys, the stress-life (S/N) properties of were markedly different. As in more traditional crystalline metallic alloys, the crack propagation mechanism in the metallic glass was associated with alternating blunting and resharpening of the crack tip as evidenced by striations on fatigue fracture surfaces. Alternatively, during S/N tests flaws apparently initiated quite easily due to the lack of microstructural barriers which would normally provide local crack-arrest points, thereby giving rise to poor S/N properties.

14. SUBJECT TERMS
Bulk amorphous metal, stress-life (S/N) Tests, crack propagation mechanism

15. NUMBER OF PAGES
15

16. PRICE CODE

17. SECURITY CLASSIFICATION OF REPORT	18. SECURITY CLASSIFICATION OF THIS PAGE	19. SECURITY CLASSIFICATION OF ABSTRACT	20. LIMITATION OF ABSTRACT
UNCLASSIFIED	UNCLASSIFIED	UNCLASSIFIED	

Final Technical Report

to

U.S. Air Force Office of Scientific Research

on

MICROMECHANISMS OF FRACTURE AND FATIGUE-CRACK GROWTH IN BULK METALLIC GLASS ALLOYS

for period 1 May 1997 to 31 December 1997

submitted to

U.S. Air Force Office of Scientific Research
Directorate of Aerospace and Materials Research
AFOSR/NA
110 Duncan Avenue, Suite B115
Bolling Air Force Base
Washington, D.C. 20322
Attention: Dr. Spencer Wu

submitted by

C. J. Gilbert and R. O. Ritchie
Department of Materials Science and Mineral Engineering
University of California, Berkeley, California 94720-1760

March 1998

TABLE OF CONTENTS

Page

MICROMECHANISMS OF FRACTURE AND FATIGUE-CRACK GROWTH IN BULK METALLIC GLASS ALLOYS

C. J. Gilbert and R. O. Ritchie

(Grant No. F496209-97-1-0365)

FOREWORD

ABSTRACT

The recent development of metallic alloy systems which can be processed with an amorphous structure over large dimensions, specifically to form metallic glasses at low cooling rates (~10 K/s), has permitted novel measurements of important mechanical properties. These include, fatigue-crack growth and fracture toughness behavior, representing the conditions governing the subcritical and critical propagation of cracks. In the present study, bulk plates of a $Zr_{41.2}Ti_{13.8}Cu_{12.5}Ni_{10}Be_{22.5}$ alloy, machined into 7 mm thick, 38 mm wide compact-tension specimens and fatigue precracked following standard procedures, revealed fracture toughnesses in the fully amorphous structure of K_{Ic} ~ 55 MPa√m, i.e., comparable with that of a high-strength steel or aluminum alloy. However, annealing to induce partial and full crystallization was found to result in a drastic reduction in fracture toughness to ~1 MPa√m, i.e., comparable with silica glass. Under cyclic loading, whereas crack-propagation behavior of the bulk amorphous metal was similar to that observed in traditional steel and aluminum alloys, the stress-life (S/N) properties of were markedly different. As in more traditional crystalline metallic alloys, the crack propagation mechanism in the metallic glass was associated with alternating blunting and resharpening of the crack tip as evidenced by striations on fatigue fracture surfaces. Alternatively, during S/N tests flaws apparently initiated quite easily due to the lack of microstructural barriers which would normally provide local crack-arrest points, thereby giving rise to poor S/N properties.

MICROMECHANISMS OF FRACTURE AND FATIGUE-CRACK GROWTH IN BULK METALLIC GLASS ALLOYS

1. INTRODUCTION

The recent development of techniques for the processing of metallic glasses in bulk form [1] permits for the first time the measurement of important mechanical properties in amorphous metals, in particular the fatigue and fracture characteristics. Previous work on metallic glasses has invariably been confined to very thin ribbons or wires, thus making measurements difficult [2,3]; few results are thus available on the toughness and cyclic crack growth or stress/life properties of these alloys. Accordingly, the objective of the current study is to quantify the fracture toughness, fatigue-crack growth, and stress/life properties of a recently developed bulk metallic glass alloy, $Zr_{41.2}Ti_{13.8}Cu_{12.5}Ni_{10}Be_{22.5}$ (nominal composition in at.%). We present results characterizing the hardness, fracture toughness and fatigue resistance of this alloy; in addition, we compare properties in the fully amorphous structure with that of partially and fully crystallized structures in the same alloy.

2. EXPERIMENTAL PROCEDURES

2.1 Material and Microstructure

As-received plates of the alloy, processed using methods described elsewhere [1], were found to be *fully amorphous*. By heat treating at 633 K for 12 h *in vacuo*, just above the glass-transition temperature ($T_g \sim 625$ K), a *partially crystallized* structure was formed. This consisted of the amorphous matrix containing ~3 to 5 nm nanocrystallites of a Cu-rich, Ti-rich fcc phase with an average spacing of ~20 nm between nanocrystals; the volume fraction of the crystalline fcc phase was estimated from x ray and transmission electron microscopy data to be less than 5% of the sample [4,5]. By heat treating at 723 K for 24 h *in vacuo*, a *fully crystallized* multiphase microstructure was obtained, containing a Laves phase with the hcp "MgZn₂-type" structure [5], a phase with the "Al₂Cu-type" structure, and at least one additional unidentified phase. The degree of crystallinity for each structure is indicated by the x ray diffraction data in Fig. 1.

2.2 Fracture Toughness and Fatigue-Crack Propagation

Fracture toughness and fatigue-crack growth rate properties were determined in a controlled room-air environment (22°C, 45% relative humidity) on 7 mm thick, 38 mm wide compact-tension C(T) specimens, machined from the bulk plates. Specimens were cycled under stress intensity (K) control, with a test frequency of 25 Hz (sinusoidal waveform) at a constant load ratio (ratio of minimum to maximum load) of $R = 0.1$, using computer-controlled, servo-hydraulic mechanical testing machines, in general accordance

with ASTM standard E647. To obtain a wide spectrum of growth rates, samples were first cycled with a decreasing stress-intensity range (at a normalized K-gradient of 0.2 mm^{-1}) until measured growth rates were less than 10^{-10} m/cycle; the value of the stress-intensity range at this point was used to operationally define the fatigue threshold stress intensity (ΔK_{TH}), below which long cracks are essentially dormant. After threshold determination, specimens were cycled under increasing ΔK conditions with the same K-gradient in order to determine growth rates up to ~10^{-8} m/cycle.

Crack initiation was facilitated using a half-chevron shaped starter notch; prior to data collection, samples were fatigue pre-cracked for several millimeters beyond this notch. Thereafter, crack lengths were continuously monitored using unloading elastic-compliance measurements with a 350 Ω strain gauge attached to the back-face of the specimen; crack lengths were also checked periodically using a traveling microscope. Optical and compliance measurements were always found to be within 2%. Data are presented in terms of the growth rate per cycle, da/dN, as a function of the alternating stress intensity, ΔK ($= K_{max} - K_{min}$), the latter being computed using standard linear-elastic handbook solutions.

Following growth-rate measurements, fracture toughness, K_{Ic}, values were determined by monotonically loading the fatigue precracked specimens to failure; procedures were in general accordance with ASTM standard E399. However, fatigue cracking was unstable in the partially and fully crystalline structures due to their extreme brittleness; correspondingly, toughness values here were obtained using Vickers indentation methods, with measurements averaged from at least five indents under an indentation load of 49 N.

2.3 Stress/Life Behavior

As-received (7 mm thick, 40 × 40 mm) plates of the $Zr_{41.2}Ti_{13.8}Cu_{12.5}Ni_{10}Be_{22.5}$ (at%) fully amorphous alloy, were machined into 3 × 3 × 50 mm rectangular beams for S/N testing. Fatigue lifetimes, N_f, were measured over a range of cyclic stresses by cycling in four-point bending, with an inner span, S_1, and outer span, S_2, of 10.2 mm and 20.3 mm, respectively. Specimens, which had been previously polished to a ~1 μm surface finish, were cycled under load control at a frequency of 25 Hz (sinusoidal waveform) in a room air environment (25°C, ~45% relative humidity) on a servohydraulic mechanical test frame. The ratio of the minimum to maximum load, $R = \sigma_{min}/\sigma_{max}$, was maintained at 0.1 for all tests.

Stresses were calculated at the tensile surface within the inner span from $\sigma = 3P(S_2 - S_1)/2bh^2$, where P is the applied load, b the specimen thickness, and h the specimen height. A total of 21 beams were tested at maximum stresses ranging from 100 MPa to 1800 MPa (just below the tensile failure stress, $\sigma_u \sim 1890$ MPa [6]), with multiple measurements made at each stress when possible. Tests were terminated in cases were failure had not occurred after 2×10^7 cycles (~9 days at 25 Hz). Fracture

surfaces of selected beams were examined after failure via both optical and scanning electron microscopy (SEM) in order to discern the origin and mechanisms of failure. Stress/life data are presented in terms of the stress amplitude, $\sigma_a = \frac{1}{2}(\sigma_{max} - \sigma_{min})$, normalized by the tensile strength, σ_u, plotted as a function of the number of cycles to failure, N_f, where one cycle is defined as a full stress reversal.

3. RESULTS AND DISCUSSION

3.1 Fracture Toughness and Fatigue-Crack Propagation

Results indicated that the fracture toughness of the amorphous alloy was 55 (±5.0) MPa√m. Thermal exposure resulting in partial or full crystallization, however, led to approximately a 50-fold reduction in K_{Ic} values to 1.21 (±0.04) and 1.04 (±0.05) MPa√m, respectively (Fig. 1). Whereas the toughness of the metallic glass is comparable to that of a typical (crystalline) aluminum or high-strength steel alloy, the toughness after partial or full crystallization is comparable to that of silica glass or very brittle ceramics. On the other hand, Vicker's hardness values marginally increased from 5.37 (±0.08) GPa in the glass to 6.04 (±0.04) and 6.35 (±0.10) GPa, respectively, in the partially and fully crystallized structures.

This drastic embrittlement upon crystallization meant that fatigue cracking was not observed in these structures; any attempt to grow stable cracks from the machined notches led to catastrophic failure of the sample. Such behavior is typical of very brittle (untoughened) ceramics, and is consistent with the precipitous drop in toughness on crystallization. However, stable fatigue-crack growth behavior was characterized in the amorphous structure under cyclic loading. Results in the form of growth rates as a function of ΔK are plotted in Fig. 2 and compared to results for a range of ceramic and metallic materials, including polycrystalline alumina, high-strength steel, and high-strength aluminum alloys. Note that these data pertain to plane-strain conditions (based on a yield strength of ~1890 MPa [6]), unlike previous data for metallic glasses which were measured on very thin sheets [7,8]. It is apparent that cyclic crack growth rates in the amorphous metal lie between that of high-strength steel and aluminum alloys. When regression fit to a simple Paris power-law equation [9]:

$$da/dN = C \, \Delta K^m , \qquad (1)$$

the crack-growth scaling constants are found to be $C = 1.46 \times 10^{-11}$ and $m = 2.7$ (units: m/cycle, MPa√m). The exponent m is typical of ductile metallic alloys, which usually lie between 2 to 4 over this regime of growth rates; this is in contrast to brittle materials like alumina where m is typically 20 or higher [10]. The threshold for fatigue-crack growth in the metallic glass, ΔK_{TH}, is ~3 MPa√m; this is again comparable to many aluminum and steel alloys, although it does not appear to be as distinct as in the polycrystalline metals.

The corresponding fracture surfaces display a morphology quite distinct from anything seen in crystalline metals, with the fracture surface roughness increasing markedly with increasing crack velocity. Surfaces vary from a rough morphology exhibiting ridge-like features in the fast-fracture region (Fig. 3a) to a mirror-like surface in the near-threshold fatigue region. However, closer examination of the fatigue surfaces, particularly in the higher growth-rate region, reveal clear evidence of classic fatigue striations (Fig. 3b), i.e., "beach markings" parallel to the crack front representing the cycle-by-cycle advance of the crack. Indeed, such striations have been reported in the past for the fatigue of metallic glasses in thin sheet [7,8].

The mechanism of striation formation in amorphous alloys is as yet unclear. However, in ductile crystalline metals, some degree of irreversible slip at the crack tip is required alternately to blunt the crack on the loading cycle and subsequently re-sharpen it on unloading [11], and tensile experiments in this [6] and other amorphous metals [2,3] indicate that slip bands readily form. Models for striation formation [11] indicate that growth rates should scale with the range of crack-tip opening displacement, $\Delta\delta$, which using simple continuum mechanics arguments is given by [11]:

$$\Delta\delta = \beta \frac{\Delta K^2}{\sigma_Y E'} \ , \qquad (2)$$

where σ_Y is the flow stress, $E' = E$ (Young's modulus) in plane stress and $E/(1-v^2)$ in plane strain (v is Poisson's ratio), and β is a scaling constant (~0.01 to 0.1 for mode I crack growth) which is a function of the degree of slip reversibility and elastic-plastic properties of the material. The fact that Eq. 2 provides a reasonable description of the experimentally measured growth rates for the metallic glass, with $m \sim 2.7$ and $\beta \sim 0.01$ (Fig. 2), together with the presence of fatigue striations on the fracture surfaces (Fig. 3b), strongly suggests a mechanism for crack advance involving repetitive blunting and resharpening, i.e., a mechanism similar to that commonly observed in crystalline metals.

3.2 Stress/Life Behavior

The normalized stress amplitude, σ_a/σ_u, is plotted as a function of cycles to failure, N_f, for the $Zr_{41.2}Ti_{13.8}Cu_{12.5}Ni_{10}Be_{22.5}$ alloy in Fig. 4. Results are compared with that for 300-M high strength steel [12] and the 2090-T81 aluminum-lithium alloy [13]. It is clear from Fig. 4 that despite the similarity in crack-growth properties of bulk amorphous metals to polycrystalline metals (Fig. 2), the S/N properties are very different. Not only are fatigue lifetimes significantly shorter in the metallic glass (at a given value of σ_a/σ_u), but lifetimes exhibit a much lower dependence on the stress amplitude. For example, by fitting the S/N data to the simple (Basquin) equation $(\sigma_a)^n N_f$ = constant, fatigue lives in the metallic glass are proportional to $(\sigma_a)^{-3.4}$, compared to the more common result of $(\sigma_a)^{-10}$ in steel and aluminum. Moreover, whereas steel and aluminum alloys generally display a fatigue limit or 10^7-cycle endurance strength at values of σ_a/σ_u between 0.3 and 0.5 (for $R = 0.1$), no such fatigue limit can be detected in the metallic glass until σ_a/σ_u

drops below ~0.04. These results are consistent with previous studies on rapidly-quenched thin ribbons of metallic glass which also indicate a low dependence of fatigue life on the applied stress amplitude [8,14].

Careful optical examination of fatigue fracture surfaces indicates that cracking originates from a corner of the beam at the tensile face of the specimen, with the extent of stable fatigue-crack propagation increasing with life. At long lives, where $N_f > 10^6$ cycles, the fatigue fracture surface contains large regions which display a mirror-like appearance with no detectable evidence of topographical features. Indeed, the crack-propagation studies revealed that the roughness of the fatigue surfaces in this alloy progressively diminishes with decreasing growth rates, leading to a mirror-like morphology at near-threshold levels (i.e., at $da/dN \sim 10^{-10}$ m/cycle). The origin of such behavior is unknown but almost certainly involves extensive sliding crack-surface interference between the mating crack surfaces. Detailed SEM analysis of the fracture surfaces indicate a very distinct transition from stable fatigue-crack propagation to overload fracture. For example, the montage in Fig. 5 (representing an area ~70 × 110 μm) indicates striation-type growth in the fatigue region on the left, followed by an abrupt change to a vein morphology characteristic of overload fracture in metallic glasses [3].

The results in Figs. 2 and 4 present an interesting contrast between crystalline and amorphous metals. Whereas the crack-propagation properties are similar in the two classes of materials (with respect to the presence of fatigue striations and the dependence of growth rates on ΔK), the S/N behavior is markedly different. Total life is far less dependent upon the applied stress amplitude and the fatigue limit is smaller by an order of magnitude. This implies that mechanistically the fatigue properties of crystalline and amorphous metals differ significantly with respect to crack *initiation*, or more precisely in the nucleation of crack growth. This may be associated with the easier natural initiation of a fatigue crack, e.g., via "slip-band" formation [6,7], although nothing is known about the initiation mechanisms in these materials at this time. However, since the fatigue limit can be equated with the critical stress for crack initiation or more generally for an initiated (small) crack to "overcome" some microstructural barrier (e.g., a grain boundary) [15], we may presume that the markedly lower fatigue limits in the amorphous alloys may be associated with a lack of microstructure which would normally provide local arrest points.

4. CONCLUSIONS

Based on an experimental study of the cyclic fatigue behavior of a bulk metallic glass alloy, $Zr_{41.2}Ti_{13.8}Cu_{12.5}Ni_{10}Be_{22.5}$ (at%), involving both crack propagation (using precracked C(T) specimens) and stress/life (using nominally crack-free, unnotched beams) studies, the following conclusions can be made:

1. The *bulk* metallic glass, $Zr_{41.2}Ti_{13.8}Cu_{12.5}Ni_{10}Be_{22.5}$, has a high fracture toughness of ~55 MPa√m, which is drastically reduced by a factor of over 50 upon crystallization, i.e., from levels comparable to high-strength steel and aluminum alloys when fully amorphous to levels comparable to brittle ceramics when partially or fully crystallized.

2. Crack-propagation behavior is similar to that observed in traditional ductile crystalline alloys (e.g., high-strength steels and aluminum alloys), both in terms the dependence of growth rates on the applied stress-intensity range and in the presence of ductile striations on fatigue fracture surfaces.

3. Conversely, the stress-life behavior of the metallic glass (at $R \sim 0$) was very different from that observed in the crystalline alloys. Fatigue lifetimes were much shorter in the amorphous alloy and exhibited a far lower dependence on the applied stress range; moreover, no evidence of a fatigue limit could be detected until stress amplitudes dropped below ~1/25 of the tensile strength.

4. Given the similarity in crack-growth behavior but the very different stress/life properties, the prime distinction in the cyclic fatigue behavior of ductile crystalline and bulk amorphous metals appears to be associated with crack initiation properties.

5. ACKNOWLEDGMENTS

6. REFERENCES

1. A. Peker and W. L. Johnson, Appl. Phys. Lett. **63**, 2342 (1993).

2. J. J. Gilman, J. Appl. Phys. **46**, 1625 (1975).

3. C. A. Pampillo and A. C. Reimschuessel, J. Mat. Sci. **9**, 718 (1974).

4. R. Busch, S. Schneider, A. Peker, and W. L. Johnson, Appl. Phys. Lett. **67**, 1544 (1995).

5. S. Schneider, P. Thiyagarajan, and W. L. Johnson, Appl. Phys. Lett. **68**, 493 (1996).

6. H. A. Bruck, T. Christman, A. J. Rosakis, and W. L. Johnson, Scripta. Met. **30**, 429 (1994).

7. L. A. Davis, J. Mat. Sci. **10**, 1557 (1975).

8. T. Ogura, T. Masumoto, and K. Fukushima, Scripta Met. **9**, 109 (1975).

9. P. C. Paris and F. Erdogan, J. Bas. Eng. **85**, 528 (1963).

10. C. J. Gilbert, R. H. Dauskardt, and R. O. Ritchie, J. Am. Ceram. Soc. **78**, 2291 (1995).

11. F. A. McClintock, Boeing Technical Report (1967), cited in R. M. N. Pelloux, Trans. ASM **62**, 281 (1969).

12. W. F. Brown, Jr., Aerospace Structural Metals Handbook, Code 1224, Metals and Ceramics Information Center, 1-30 (1989).

13. K. T. Venkateswara Rao and R. O. Ritchie, Int. Mat. Rev. **37**, 153 (1992).

14. L. A. Davis, J. Mat. Sci. **11**, 711 (1976).

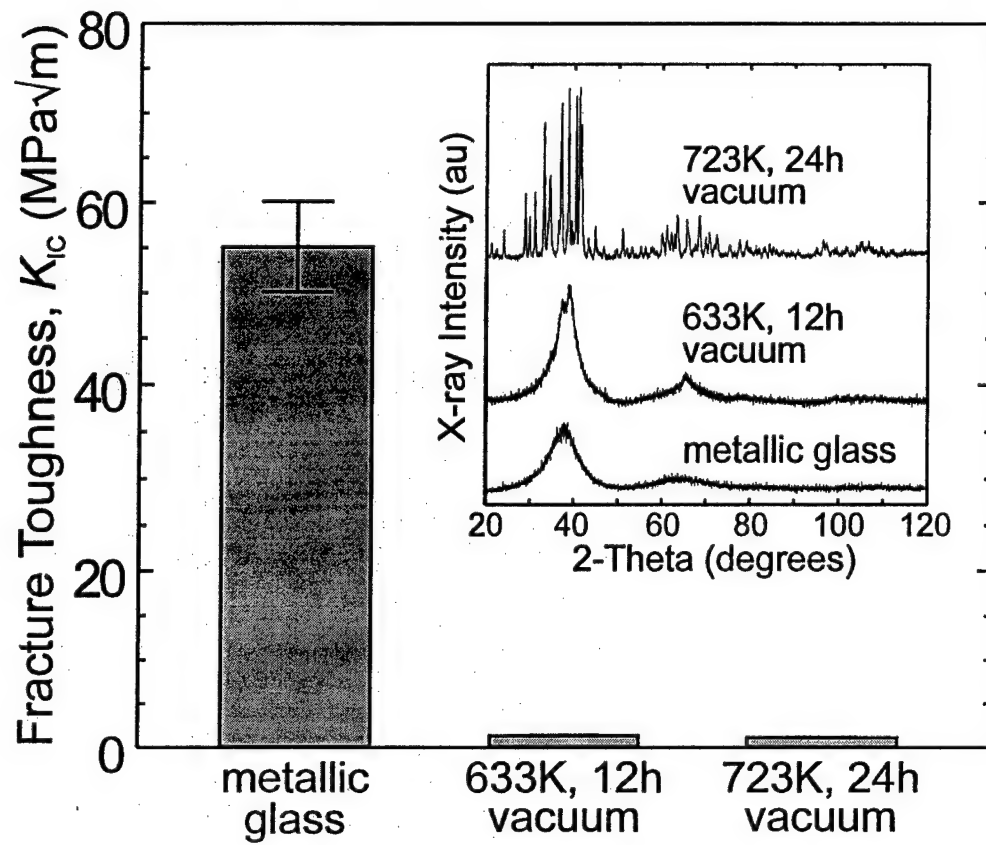15. K. J. Miller, Fat. Fract. Eng. Matls. Struct. **10**, 93 (1987).

Fig. 1. While the fracture toughness of the amorphous alloy was ~55 MPa√m, thermal exposure resulting in partial or full crystallization leads to a 50-fold reduction in K_{Ic} values to ~1.21 MPa√m, respectively. X-ray diffraction data corresponding to each of these microstructures are included in the inset.
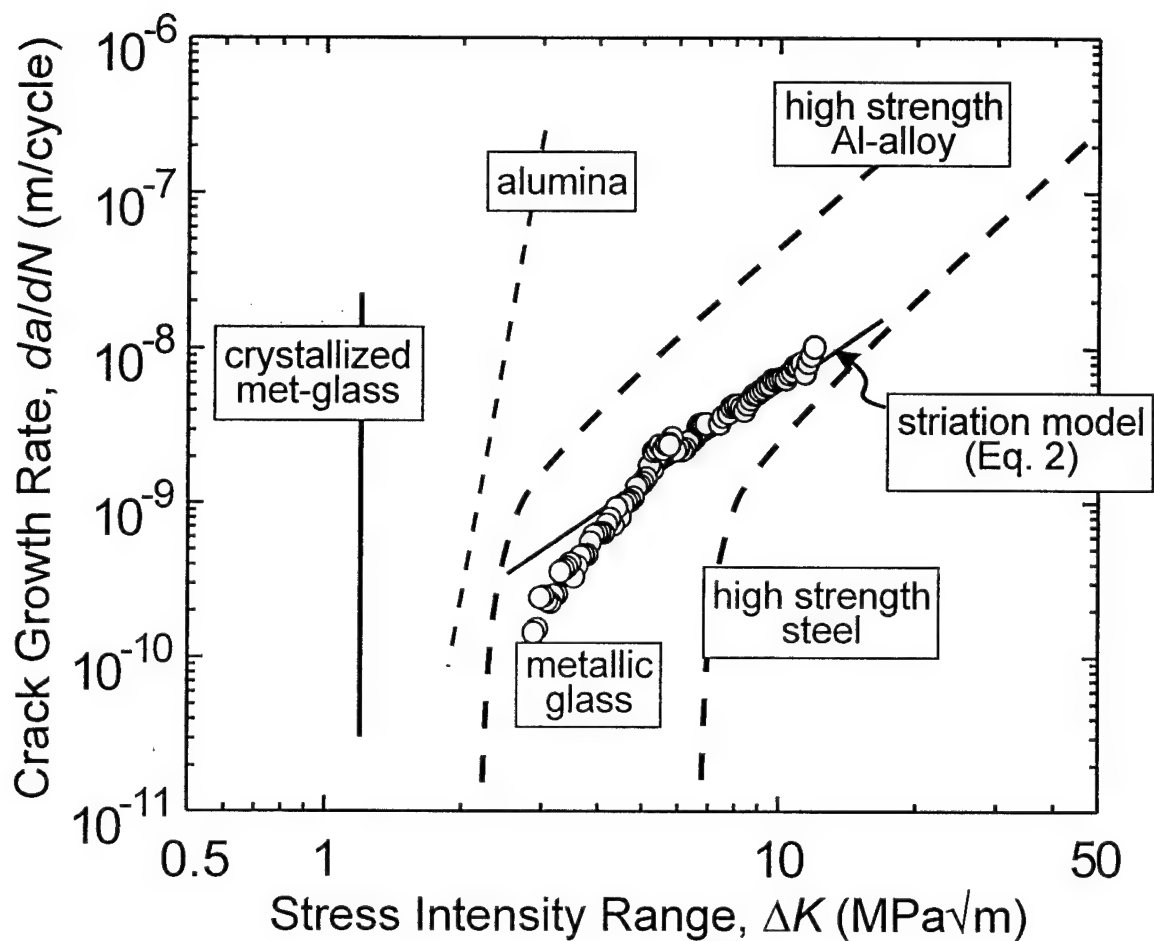
Fig. 2. Fatigue-crack growth rate, *da/dN*, is plotted as a function of stress-intensity range, ΔK, for the amorphous and crystallized $Zr_{41.2}Ti_{13.8}Cu_{12.5}Ni_{10}Be_{22.5}$ alloy. Data are compared to a range of engineering materials, including fine-grained alumina, 2.25Cr-1Mo steel and 2124 aluminum alloy. Growth rates in the amorphous structure were found to be comparable to that in many ductile crystalline metals such as high-strength aluminum alloys and steels.
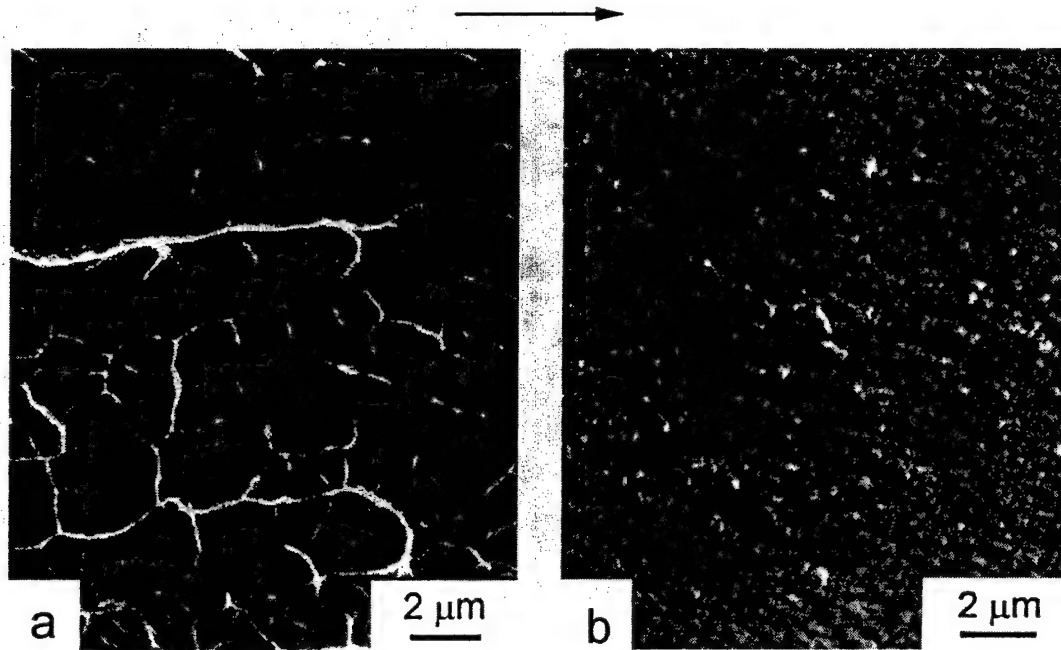
Fig. 3. Scanning electron micrographs of fracture surfaces developed during (a) overload fracture and (b) fatigue-crack growth. Arrow represents direction of crack extension.
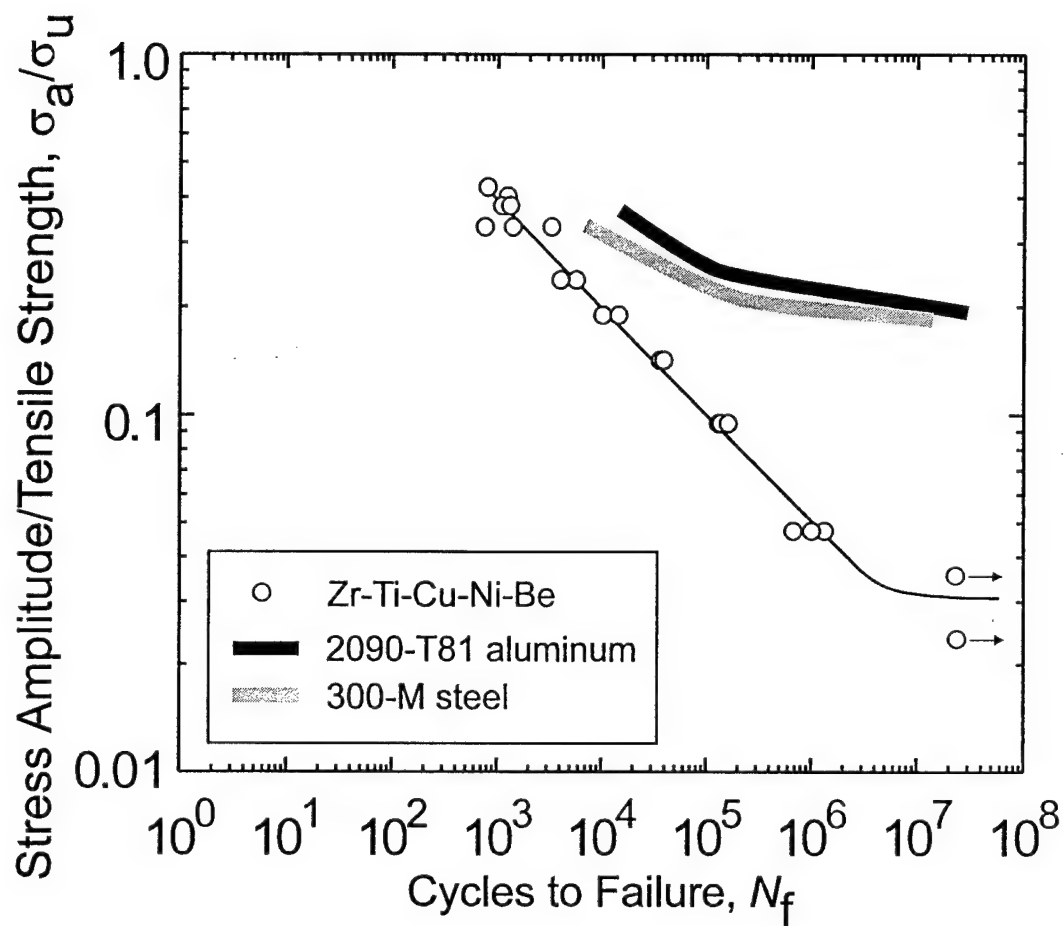
Fig. 4. Cycles to failure, N_f, plotted as a function of the applied stress amplitude, σ_a, normalized by the tensile strength, σ_u. Data for the bulk amorphous alloy are compared to behavior in high strength steel and aluminum alloys.
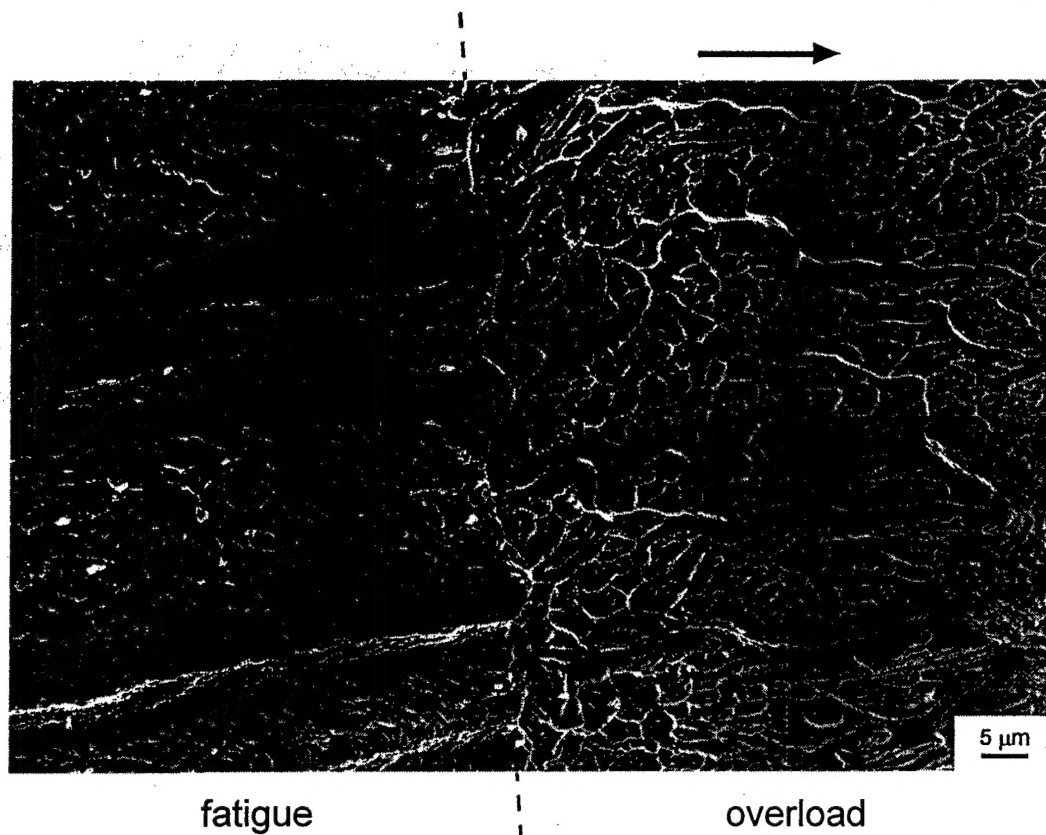
Fig. 5: Scanning electron micrograph of the boundary between fatigue and final fracture on the surface of an S/N beam broken under cyclic loads ($N_f \sim 1.3 \times 10^6$ cycles, $\sigma_a =$ 90 MPa). The arrow represents the nominal direction of crack propagation, and the dotted line marks the boundary between fatigue and overload fracture.

7. PROGRAM ORGANIZATION AND PERSONNEL

The work described in this report was performed in the Department of Materials Science and Mineral Engineering, University of California at Berkeley, under the supervision of Dr. R. O. Ritchie, Professor of Materials Science, and Dr. C. J. Gilbert, Postdoctoral Research Engineer, and aided by a graduate student research assistant working for her Ph.D. degree.

    i)   Professor R. O. Ritchie, Principal Investigator
           Department of Materials Science and Mineral Engineering

    ii)   Dr. C. J. Gilbert, Postdoctoral Research Engineer
           Department of Materials Science and Mineral Engineering

    iii) Valeska Schroeder, Graduate Student Research Assistant
           Department of Materials Science and Mineral Engineering

    iv) Julian Lippmann, Undergraduate Research Assistant
           Department of Materials Science and Mineral Engineering

8. PUBLICATIONS

8.1 Refereed Journals

1. C. J. Gilbert and R. O. Ritchie, "Fracture Toughness and Fatigue-Crack Propagation in a Zr-Ti-Ni-Cu-Be Bulk Metallic Glass," *Appl. Phys. Lett.* **71**(4), July 1997, pp. 476-78.

2. C. J. Gilbert, J. M. Lippman, and R. O. Ritchie, "Fatigue of Zr-Ti-Cu-Ni-Be Bulk Amorphous Metal: Stress/Life and Crack-Growth Behavior," *Scripta Mater.* **38**(4), Jan. 1998, pp. 537-42.

8.2 Presentations

1. C. J. Gilbert and R. O. Ritchie, "Fracture Toughness and Fatigue-Crack Propagation in a Zr-Ti-Ni-Cu-Be Bulk Metallic Glass," presented at the Annual Meeting of the Metals, Minerals, and Materials Society, Indianapolis, IN, September 1997.

9. DISTRIBUTION LIST

AFOSR/NA
ATTN: Spencer Wu
110 Duncan Avenue, Suite B115
Bolling Air Force Base
Washington, D.C. 20332-8080

AFWAL/MLLM
ATTN: Branch Chief
Wright-Patterson AFB
Dayton, OH 45433

AFWAL/MLLS
ATTN: Branch Chief
Wright-Patterson AFB
Dayton, OH 45433

AFWAL/MLLN
ATTN: Branch Chief
Wright-Patterson AFB
Dayton, OH 45433

Dr. Hugh R. Gray
NASA Lewis Research Center
Materials and Structures Division
21000 Brookpark Rd.
Cleveland, OH 44135